05.1;06.4

Dynamics of deformation bands initiated by impact of an indenter on the surface of aluminum−magnesium alloy

© A.A. Shibkov, A.E. Zolotov, A.A. Denisov, M.F. Gasanov

Tambov State University, Tambov, Russia
E-mail: shibkov@tsu.tmb.ru

The dynamics of macrolocalized deformation bands generated by the impact of a Vickers indenter on the surface of an AlMg6 aluminum−magnesium alloy deformed under creep conditions was studied by high−speed video recording and acoustic emission methods. It has been established that these bands are the trigger for the development of a macroscopic jump in plastic deformation on the creep curve. It is shown that in alloys exhibiting the Portevin−Le Chatelier effect it is necessary to take into account the initiation and propagation of deformation macrobands during surface erosion damage and to estimate the volume and morphology of the plastic zone during impact microindentation of a deformable alloy.

Keywords: intermittent deformation, deformation band, impact, indenter, aluminum−magnesium alloy.

Aluminum−magnesium alloys with the magnesium content of 3−6% are widely used in aerospace industry, ship building, automobile industry and chemical engineering. In the technologically important ranges of deformation rates and test temperatures, these alloys exhibit an intermittent deformation manifesting itself in repetitive stress jumps occurring during deformation with the preset rate $\dot{\varepsilon}_0 = $ const at a stiffness testing machine (the Portevin−Le Chatelier effect), during loading with the preset rate $\dot{\sigma}_0 = $ const (the Savar−Masson effect), and under the creep conditions $\sigma_0 = $ const (staircase creep) [1]. In all the mentioned cases, deformation jumps result from spontaneous generation and propagation of macrolocalized deformation bands negatively affecting mechanical and corrosion properties of the alloys, for instance, reducing their plasticity and corrosion resistance, and, possibly, causing sudden damages. Investigation of the effect of external impacts on intermittent deformation and band formation in commercial aluminum alloys were started in works [2,3] devoted to the influence of pulsed laser radiation [2] and chemically aggressive medium [3]. The goal of this work was to study the influence of the indenter impact against the surface of the deformable aluminum−magnesium alloy on the deformation bands dynamics and morphology and subsequent development of the macroscopic jump in plastic deformation.

As the test sample, alloy AlMg6 (Al−6.15 mass% Mg−0.65 mass% Mn−0.25 mass% Si−0.21 mass% Fe) was used. Samples were cut from a cold−rolled sheet in the form of bilateral blades with the effective area of $6 \times 3 \times 0.5$ mm, annealed for an hour at the temperature of $450°$C, and quenched in air. The scheme of tension under the intermittent creep conditions is described in detail in [4]. Tension at a soft testing machine was performed first in the mode of loading with the rate of $\dot{\sigma}_0 = 1$ MPa/s up to the stress of $\sigma_0 = 260$ MPa, and then in the creep mode. The band dynamics was studied by acoustic emission (AE) and rapid video recording with the speed of up to 20 000 fps (frames per second) using high−speed digital camera VS-FASTG6 (Videoscan) mounted on the side of the flat sample surface opposite to the indenter. An acoustic channel comprising acoustic emission sensor Zetlab BC 601 and preamplifier AEP5 (Vallen-Systeme) detected the AE signals in the frequency band from ~ 30 to ~ 600 kHz. The sample surface was subject to impacts from the Vickers indenter suspended on a light bronze tape (see the Fig. 1 inset); the indenter was triggered by exploding a compact charge of explosive substance (ES) with a pulse of infrared laser (YLP-1-100-50-50-HC-RG). The force response was detected by tensometer (Zemic H3-C3-100 kg-3B), deformation was measured with a laser triangulation sensor (Riftec) having sensitivity of 1.5μm in the frequency band of up to 2 kHz.

Fig. 1 presents synchronous records of signals from the deformation (1) and acoustic−emission (2) sensors and tensometer (3), which were induced by the Vickers indenter impact against the center of the sample effective area during its tension under the creep conditions at $\sigma_0 = 260$ MPa. The indenter made the impact in $\tau_{imp} = 60$ s after reaching the creep mode. In the absence of external effects at the given applied stress, the creep curve jump takes place spontaneously in $\tau \sim 100$ s. As the figure shows, the indenter impact initiates a „precocious" development of the deformation jump with amplitude $\Delta\varepsilon \approx 4\%$ (curve 1 in Fig. 1), which is accompanied by characteristic repetitive bursts of AE signals (curve 2) and stress drops in the force response (curve 3). Amplitude of the first AE burst occurring simultaneously with the indenter impact exceeds considerably amplitudes of subsequent AE signals
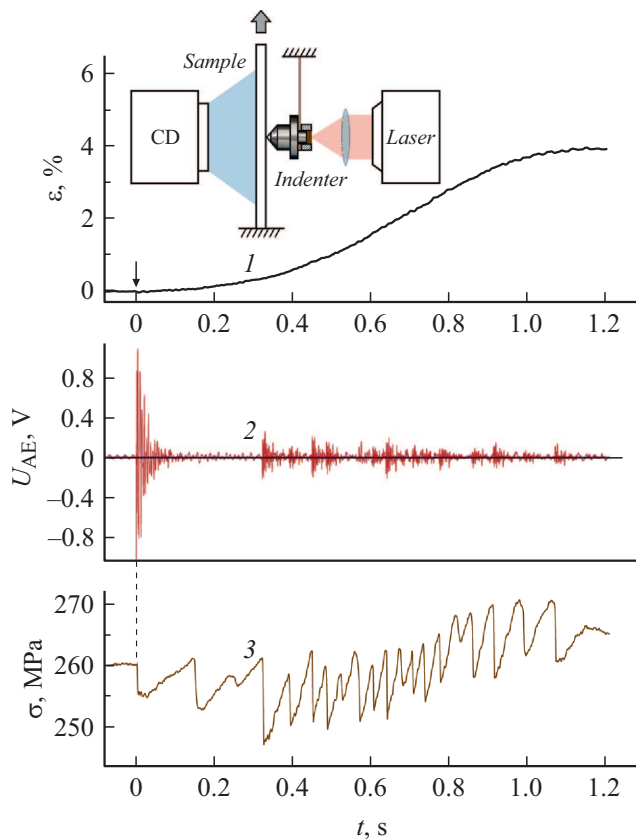
Figure 1. Synchronous records of the deformation (*1*), acoustic (*2*) and force (*3*) responses to the Vickers indenter impact against the surface of the alloy AlMg6 flat sample initiated by exploding the ES charge installed in the indenter tail part. The arrow indicates the moment of impact. The inset presents the experimental setup.

and is to a high extent caused by strictly the indenter impact against the sample surface. Further AE bursts and stress drops are associated with generation and expansion of the deformation bands initiating the deformation jump development. Correlation of these time series with the deformation band dynamics is described in detail in [4,5].

Data from 20 000 fps video recording shows that in the center of effective area on the surface opposite to the indenter first there appears a mark (indicated with the arrow in Fig. 2) in the form of a cross or straight section 0.1−0.3 mm long from which two conjugated deformation bands are then (during 1−2 frames or 50−100 μs) „shot" through the sample cross−section at the angles of ±30° to the sample normal cross−section. The AE signal shape shows that the first signal maximum corresponds to the moment when the mark appears, while the AE signal onset corresponds to the previous frame where the mark is still absent (Fig. 2). As per [5], the AE signal amplitude matches with the moment when the embryo band reaches the opposite surface of the flat sample. Data from the high−speed video recording and AE signal measurements show that the mark appears when the surface opposite

to the indenter is reached by the tip of deformation band generated by the indenter impact, while the impact onset is fixed by the AE signal start, which gives the upper estimate of the band propagation time $\Delta t = 50\,\mu s$ and lower estimate of its tip velocity $v_t \approx w/\Delta t \sim 10\,m/s$, where $w = 0.5\,mm$ is the sample thickness. Notice that in the case of intermittent deformation the bands propagate in the plane of maximal tangent stresses directed at the angle $\beta \approx 56-63°$ to the tension axis [5,6] (in an isotropic plastically deformable material, this angle corresponds to condition $\mathrm{tg}\,\beta = \sqrt{2}$ which gives $\beta = 54°44'$ [7]). The main (shear) crack always develops along one of the conjugated deformation bands generated by the indenter impact (see the Fig. 2 inset).

Based on the obtained results, it is possible to assume the following pattern of band formation under the indenter impact against the surface of the sample being deformed by uniaxial tension. The indenter tip as a stress concentrator generates two conjugated bands in the planes arranged at the angles of about ±30° to the sample's normal cross−section (Fig. 3). Prior to reaching the surface opposite to the indenter, band boundaries within the material bulk have an almost parabolic shape. Once the tip of one of the bands reaches the opposite surface monitored by the video camera, first a mark in the form of a straight section appears, and the crosswise mark appears after the conjugated band tip reaches the surface (Fig. 3). According to this band formation scheme, the mark proves to be precisely opposite the indenter tip, which agrees with the observations. Because of competence between the conjugated bands, one of them will dominate and become a trigger for development of the macroscopic deformation jump on the creep curve due to generation of secondary bands according to the cascade mechanism described in [4].

Let us evaluate the order of magnitude of the main characteristics of the local impact loading. The lateral video recording showed that the indenter initial velocity is $v_0 \approx 1\,m/s$, which allows estimating its kinetic energy $W = m_i v_0^2/2 \approx 2\,mJ$, where $m = 4\,g$ is the indenter weight, and also estimating mean force $\bar{P}$ during indentation as $\bar{P} = m\bar{a} = mv_0/\tau_0 \approx 80\,N$, where $\tau_0 \sim 50\,\mu s$ is the indentation time estimated based on the video record data and AE signal analysis. To estimate maximal force P_m in the contact, assume that in the case of a sharp indenter $P(h) = kh^2$ [8,9]; hence,

$$\bar{P} = h_0^{-1}\int_0^{h_0} P(h)dh = kh_0^2/3 = P_m/3,$$

where $P_m = kh_0^2$, h_0 is the contact approach, k is a constant. Thus, $P_m = 3\bar{P} \approx 240\,N$. The Vickers estimate of dynamic microhardness $HV_d = 1.854\bar{P}_m/d^2 \approx \approx 2.37\,GPa$ (where $d = 4.95\sqrt{2}h_0 \approx 250\,\mu m$ is the typical diagonal of an impress made by the Vickers indenter impact) is almost 3 times higher than the AlMg6 alloy static microhardness $HV_{st} \approx 800\,MPa$. The rate
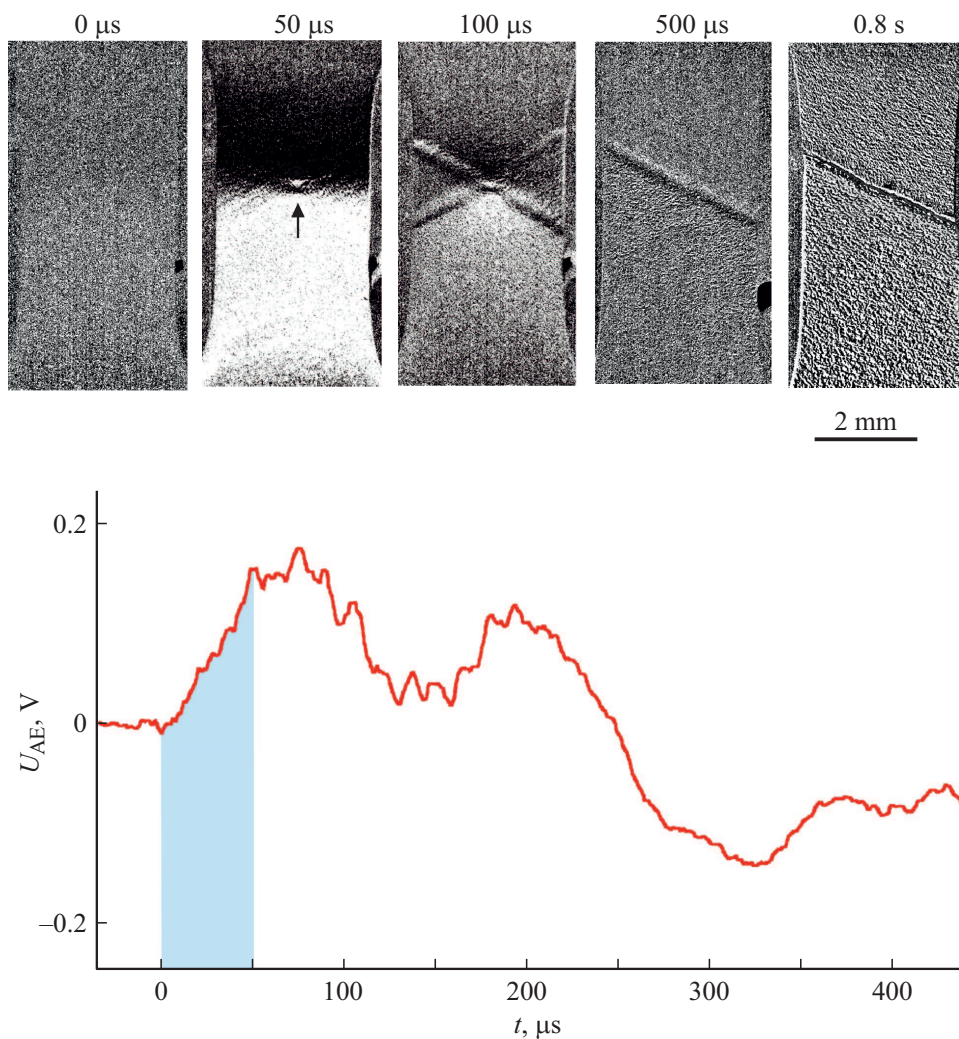
Figure 2. AE signal synchronized with the video record of the mark appearance on the surface opposite to the indenter and of the development of deformation bands initiated by the indenter impact. Time interval $\Delta t = \tau_0 = 50\,\mu s$ is marked from the impact onset moment ($t = 0$) to the moment of the mark appearance (indicated with the arrow) matching with the moment when the deformation band tip reaches the surface. The inset demonstrates the results of processing the video records from $t = 0$ to the moment of the sample damage along the deformation band at $t = 0.8\,s$.
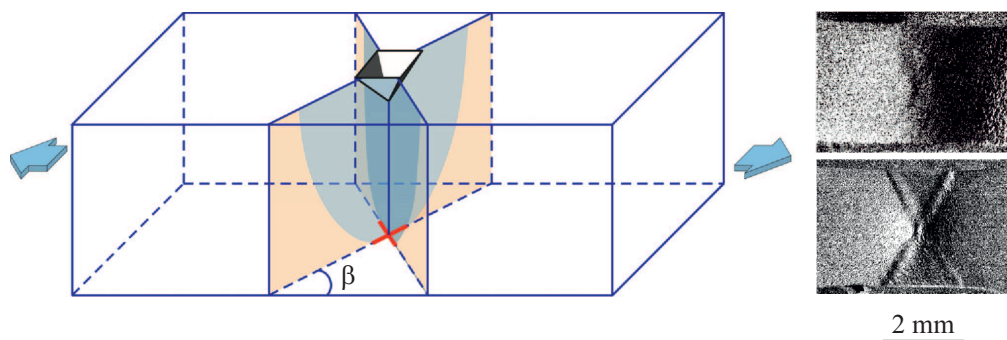

Figure 3. Schematic diagram of the embryo bands generation illustrating appearance of the mark on the sample surface opposite to the indenter. The inset presents typical images of the primary crosswise mark taken at the interval of $50\,\mu s$. Angle $\beta \approx 60°$ is the angle between the plane of maximal tangent stresses and tension axis.

of local deformation caused by the indenter impact is $\dot{\varepsilon} = h^{-1}dh/dt \sim v_0/h_0 \sim 3 \cdot 10^4\,\mathrm{s}^{-1}$, while the local loading rate is $\dot{\sigma} \approx HV_d/\tau_0 \sim 5 \cdot 10^4\,\mathrm{GPa/s}$. At the initial stages of dynamic indentation, those quantities may be significantly higher. For this range of deformation and loading rates, paper [10] has proposed an incubation time model based on the concept of „dislocation starvation" under the condition of high−rate uniaxial deformation (see also [11]) and erosion damage [12]; this concept may be applied also in the case under consideration, namely, in the case of high−rate local deformation with dynamic characteristics considerably higher that static ones. Notice that the energy of the indenter impact is comparable with the energy of an abrasive particle about 0.3 mm in size and $\sim 3\,\mathrm{g/cm^2}$ in density which flies with the speed of 250 m/s (900 km/h) typical of, e.g., volcanic ash [13] in the case of its contact interaction with the aircraft skin.

Thus, dynamic microindentation of the surface of deformed aluminum−magnesium alloy exhibiting the Portevin−Le Chatelier effect is accompanied, along with the plastic impress, by formation of latent damages in the form of macro−localized deformation bands whose subsequent evolution can result in development of the main crack.

Financial support

Conflict of interests

The authors declare that they have no conflict of interests.

References

[1] J.F. Bell, *Mechanics of solids. The experimental foundations of solid mechanics* (Springer, Berlin, 1973), vol. 1, part 2.

[2] A.A. Shibkov, A.E. Zolotov, M.F. Gasanov, M.A. Zheltov, K.A. Proskuryakov, Phys. Solid State, **60** (9), 1674 (2018). DOI: 10.1134/S1063783418090299.

[3] A.A. Shibkov, M.F. Gasanov, R.Yu. Koltsov, A. A. Denisov, Tech. Phys. Lett., **45** (8), 746 (2019). DOI: 10.1134/S106378501908013.

[4] A.A. Shibkov, M.F. Gasanov, M.A. Zheltov, A.E. Zolotov, V.I. Ivolgin, Int. J. Plast., **86**, 37 (2016). DOI: 10.1016/j.ijplas.2016.07.014

[5] A.A. Shibkov, M.A. Lebyodkin, T.A. Lebedkina, M.F. Gasanov, A.E. Zolotov, A.A. Denisov, Phys. Rev. E, **102** (4), 043003 (2020). DOI: 10.1103/PhysRevE.102.043003

[6] D. Zhemchuzhnikova, M. Lebyodkin, D. Yuzbekova, N. Lebedkina, A. Mogucheva, R. Kaibyshev, Int. J. Plast., **110**, 95 (2018). DOI: 10.1016/j.ijplas.2018.06.012

[7] R. Hill, *The mathematical theory of plasticity* (Clarendon Press, Oxford, 1950).

[8] I.A. Garcia, E.G. Berasategui, S.J. Bull, T.F. Page, J. Neidhardt, L. Hultman, N. Hellgren, Phil. Mag. A, **82** (10), 2133 (2002). DOI: 10.1080/01418610208235723

[9] Yu.V. Kolesnikov, E.M. Morozov, *Mekhanika kontaktnogo razrusheniya* (LKI, M., 2012), s. 11. (in Russian)

[10] N. Selyutina, E.N. Borodin, Y. Petrov, A.E. Mayer, Int. J. Plast., **82**, 97 (2016). DOI: 10.1016/j.ijplas.2016.02.004

[11] N.S. Selyutina, Yu.V. Petrov, Phys. Solid State, **60** (2), 244 (2018). DOI: 10.1134/S1063783418020221.

[12] A.D. Evstifeev, Yu.V. Petrov, N.A. Kazarinov, R.R. Valiev, Phys. Solid State, **60** (12), 2358 (2018). DOI: 10.1134/S1063783418120120.

[13] F. Prata, B. Rose, *The encyclopedia of volcanoes*, 2nd ed. (Academic Press, 2015), ch. 52, p. 911. DOI: 10.1016/B978-0-12-385938-9.00052-3